Odd-even staggering in yields of neutron-deficient nuclei produced by projectile fragmentation

B. Mei,[1,2,3,*] H. S. Xu,[1] Y. H. Zhang,[1] M. Wang,[1] X. L. Tu,[1,3,4] K.-H. Schmidt,[3] Yu. A. Litvinov,[1,3,4] Z. Y. Sun,[1] X. H. Zhou,[1] Y. J. Yuan,[1] K. Blaum,[4] M. V. Ricciardi,[3] A. Kelić-Heil,[3] R. S. Mao,[1] Z. G. Hu,[1] P. Shuai,[1,5] Y. D. Zang,[1] X. W. Ma,[1] X. Y. Zhang,[1] J. W. Xia,[1] G. Q. Xiao,[1] Z. Y. Guo,[1] J. C. Yang,[1] X. H. Zhang,[1] X. Xu,[1] X. L. Yan,[1,4] W. Zhang,[1] and W. L. Zhan[1]

[1]*Institute of Modern Physics, Chinese Academy of Sciences, Lanzhou 730000, China*

[2]*Extreme Light Infrastructure-Nuclear Physics, "Horia Hulubei" National Institute for Physics and Nuclear Engineering, Str. Reactorului 30, 077125 Bucharest Magurele, Romania*

[3]*GSI-Helmholtzzentrum für Schwerionenforschung GmbH, D-64291 Darmstadt, Germany*

[4]*Max-Planck-Institut für Kernphysik, Saupfercheckweg 1, D-69117 Heidelberg, Germany*

[5]*University of Science and Technology of China, Hefei, 230026, China*

(Received 16 August 2016; published 25 October 2016)

Background: Fragment yields exhibit a strong odd-even staggering (OES). This OES has been experimentally observed in different fragmentation reactions with different projectile-target combinations. However, the experimental data are still scarce for fragments close to drip lines and the origin of this OES is not well understood.

Purpose: More experimental data are needed to explore the origin of this OES in fragment yields and to validate fragmentation reaction models, especially for nuclei close to the drip lines. To study the pronounced OES near the proton drip line, we measured the yields of $T_z = -1$ and $T_z = -3/2$ nuclei over a wide range of mass number.

Methods: The combination of a fragment separator and a storage ring at the Heavy Ion Research Facility in Lanzhou has been used to measure the yields of $T_z = -1$ and $T_z = -3/2$ fragments, produced by ^{58}Ni projectiles impinging on a beryllium target at an energy of about 463 MeV/nucleon.

Results: A very strong OES is observed in the measured yields of both $T_z = -1$ and $T_z = -3/2$ fragments. Our experimental data demonstrate that the shell structure has a significant impact on the magnitude of this OES. A comparison of different fragmentation reaction data indicates that this OES is almost independent of the projectile-target combinations and the fragmentation energy between 140 and 650 MeV/nucleon.

Conclusions: Our study reveals that the OES of fragment yields originates mainly from the OES of particle-emission threshold energies, which is very close to the OES of fragment yields when the Coulomb barrier is considered in particle-emission threshold energies.

DOI: 10.1103/PhysRevC.94.044615

I. INTRODUCTION

During the last three decades, projectile fragmentation has become a most powerful experimental method used to produce nuclei far from stability at many radioactive beam facilities (see, e.g., Refs. [1–6]). The enhancement in yields of even-Z nuclides compared to the neighboring odd-Z nuclides; namely, the odd-even staggering (OES) in fragment yields, has been experimentally investigated for various fragmentation reactions with different projectile-target combinations [1,6–27]. However, full A and Z identification was not achieved in many of the previous experiments, which were limited to only Z identification (see, e.g., Refs. [7,8,11,16,17]). In this case, the OES of fragment yields (OES-FY) can hardly be well understood by studying the OES only in element yields [15,27,28]. Previous studies, mainly focusing on the OES-FY in nuclei near the valley of β stability or in neutron-rich nuclei, indicate that this OES-FY is related to pairing correlations in the nuclear binding (separation) energies [15,20,29]. A recent experiment with full A and Z identification reveals that both pairing and shell effects have significant impact on the OES-FY of $T_z = (N - Z)/2 = -1/2$ nuclei [6]. Nevertheless, the impact of shell effects is still not clear for other nuclei much closer to the drip lines. Therefore, more experimental data are needed to explore the OES-FY in nuclei toward drip lines, which is yet poorly studied.

Theoretically, many fragmentation reaction models have been proposed to study this OES-FY (see, e.g., Refs. [15,20,26,27,29,30]). It is believed to originate in excited nuclei during the evaporation process and is dominated by nuclear structure effects, e.g., pairing [15,29], shell [6], and nuclear level densities [30]. For instance, the abrasion–ablation model considering these nuclear structure effects can partly explain the observed OES-FY for nuclei near the valley of β stability [6,15,29]. However, a quantitative reproduction of this OES-FY is not achieved, especially for nuclei far from the valley of β stability [6,15,29]. Additionally, the improved statistical multifragmentation model (ISMM) with secondary decay is not able to reproduce the observed large enhancement of the OES-FY of $T_z = -1/2$ nuclei compared with that of $T_z = 1/2$ nuclei [27]. Thus, further investigations are required to explain the origin of this OES-FY, to reproduce the measured OES-FY, and to improve theoretical predictions for the yields of exotic nuclei produced in fragmentation reactions.

*meibo@impcas.ac.cn

In this work, we quantitatively study the OES-FY along a constant T_z chain, where the impact of shell structure should become very evident, as already demonstrated in Ref. [6]. The magnitude of the OES-FY for four neighboring fragments (over a constant T_z chain) centered at $Z + 3/2$ can be calculated by the following third-order difference equation [6,15,31]:

$$D_{\text{yield}}(Z) = \tfrac{1}{8}(-1)^{Z+1}\{\ln Y(Z+3) - \ln Y(Z) - 3[\ln Y(Z+2) - \ln Y(Z+1)]\}. \quad (1)$$

$Y(Z)$ is the yield value for a particular nucleus with an atomic number Z and a given T_z. The D_{yield} calculated by Eq. (1) is a very good quantity to describe the magnitude of the OES-FY according to previous studies [6,15,31,32]. For D_{yield}, the absolute value represents the strength of this OES-FY and a positive (negative) value stands for an enhanced production of even-Z (odd-Z) nuclei.

Recently, heavy-ion storage rings have been successfully applied in the measurements of nuclear reactions for nuclear physics as well as nuclear astrophysics (see, e.g., Refs. [6,33–36]). In particular, our previous experimental study in Ref. [6] demonstrates that it is possible to measure relative yields of short-lived nuclei produced in fragmentation reactions by using a combination of an in-flight fragment separator and a heavy-ion storage ring. The measured yield data can be used to investigate nuclear structure effects in the OES-FY as well as the origin of this OES-FY observed in many fragmentation reaction experiments and to constrain fragmentation reaction models. In this work, we report on a new measurement of the OES in the yields of neutron-deficient fragments, produced by fragmenting ^{58}Ni projectiles on a beryllium target, using the same method as described in Ref. [6]. The OES-FY of $T_z = -1$ and $T_z = -3/2$ nuclei very close to the proton drip line is quantitatively investigated over a wide range of mass numbers ($A \approx 20$–54). Finally, the origin of this OES-FY in these nuclei is discussed.

II. EXPERIMENTAL DETAILS

The experiment was conducted at the Cooler Storage Ring (CSR) at the Heavy-Ion Research Facility in Lanzhou (HIRFL) [37]. The primary beam of $^{58}Ni^{19+}$ ions was accelerated by the main Cooler Storage Ring (CSRm) to an energy of about 463 MeV/nucleon. After this, $^{58}Ni^{19+}$ ions were fast extracted and focused on a 15 mm beryllium target positioned at the entrance of the second Radioactive Ion Beam Line in Lanzhou (RIBLL2). At this high energy, the produced fragments emerged from the beryllium target as bare nuclei. Produced neutron-deficient fragments were transmitted through the fragment separator RIBLL2 and injected into the experimental Cooler Storage Ring (CSRe). Finally, the injected fragments were stored in the CSRe and recorded by our detection system.

During this experiment, the CSRe was tuned into an isochronous ion-optical mode, which is necessary for the application of isochronous mass spectrometry (IMS) [38–41]. Accurate measurements of mass-to-charge ratios (m/q) of stored nuclides can be achieved in the IMS at the CSRe. In the isochronous ion-optical mode, produced fragments were injected into the CSRe at an energy corresponding to $\gamma = \gamma_t \approx 1.4$ [41,42]. γ is the relativistic Lorentz factor of fragments and γ_t is the transition energy of the CSRe. The magnetic rigidity ($B\rho$) of the RIBLL2-CSRe facility was set to 5.68 and 5.81 Tm in order to obtain the best transmission for $T_z = -3/2$ and $T_z = -1$ nuclides of interest, respectively.

In the IMS, when $\gamma = \gamma_t$ is fulfilled, the revolution times T of ions stored in the CSRe are directly related to their m/q values according to the formula [41]

$$\frac{\Delta T}{T} = \frac{1}{{\gamma_t}^2}\frac{\Delta(m/q)}{(m/q)} - \left(1 - \frac{\gamma^2}{{\gamma_t}^2}\right)\frac{\Delta v}{v}, \quad (2)$$

where v is the velocity of stored ions, because the second term on the right-hand side is negligible. A high performance time-of-flight (TOF) detector [43] was applied to accurately measure the revolution time of every ion stored in the ring. The time resolution of this detector is about 118 ps full width at half maximum (FWHM) [43]. The detection efficiency in each turn is between 20% and 70% [43], which depends on the Z of the ions and the number of ions stored simultaneously in the ring. According to our studies in Refs. [43,44], the signal amplitudes produced by ions in the TOF detector also depend on the ion's Z, which can be applied in the Z identification for nuclides with different atomic numbers. Timing signals were recorded by a digital phosphor oscilloscope DPO 71254 at a sampling rate of 50 GS/s and saved for the off-line analysis. For each injection, the recorded time was 200 μs, which corresponds to about 320 revolutions for the stored ions with a revolution time of approximately 616 ns. Therefore, ions stored in the ring were registered by the TOF detector at a very high detection efficiency of nearly 100% for each injection with roughly 320 revolutions.

III. DATA ANALYSIS

The recorded data were analyzed by the same method as described in Refs. [44–48]. One can determine the revolution time of each ion from the recorded timing signals and obtain the revolution-time spectrum from the revolution times of all ions. Figure 1 presents a typical revolution-time spectrum in the time window of $T_z = -3/2$ nuclides between ^{41}Ti and ^{53}Ni. Other $T_z = -1/2$ and $T_z = -1$ nuclides within the acceptance of about $\pm 0.2\%$ for the RIBLL2-CSRe facility are also shown. In this spectrum, the transmission efficiency of ions has not been corrected. A mass-resolving power of $m/\Delta m \sim 140\,000$ has been achieved in this experiment, which enables unambiguous A and Z identification for most of the stored ions. Although the ^{51}Co and ^{34}Ar ions cannot be resolved in Fig. 1 by their revolution times due to very similar mass-to-charge ratios, they can be resolved very well by different signal amplitudes since there is a large difference between their atomic numbers; see Ref. [44] for details.

Momentum distributions and transmission efficiencies of $T_z = -1$ and $T_z = -3/2$ nuclei can be estimated by the same method as used in our previous work [6] and in Refs. [2,49]. The transmission efficiency was calculated by using the LISE++ program [50]. The LISE++ calculations have been validated in our previous experimental study [6]. According to the

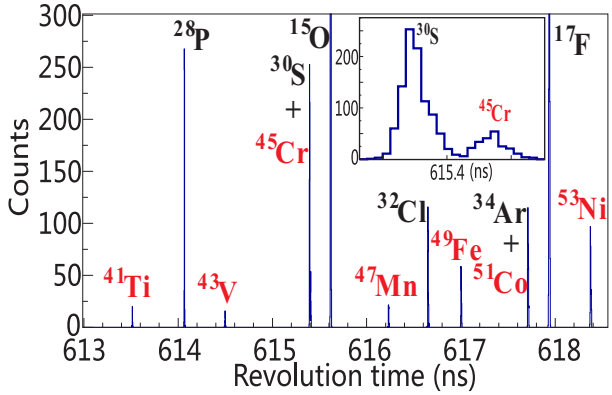

FIG. 1. The measured revolution-time spectrum in the time window of $T_z = -3/2$ nuclides of interest, which were produced in ^{58}Ni fragmentation reactions on a Be target at an energy of about 463 MeV/nucleon. The inset shows the well-resolved peaks from $^{45}Cr^{24+}$ and $^{30}S^{16+}$. This spectrum was measured with the RIBLL2-CSRe facility being optimized for the transmission of $T_z = -3/2$ nuclides centered around ^{47}Mn. Measured $T_z = -3/2$ nuclei together with their mass numbers are indicated by red letters. The upper parts of the peaks from ^{15}O and ^{17}F have been cut to clearly show other peaks of interest.

LISE++ calculations for $T_z = -1$ and $T_z = -3/2$ nuclei, the transmission efficiency varies almost smoothly with Z and does not show an odd-even staggering for nuclides along a constant-T_z chain. Decay losses of fragments are almost negligible, because the data-acquisition time of merely 200 μs is far shorter than the half-lives of all considered nuclei, which are much longer than 50 ms.

IV. RESULTS AND DISCUSSION

A. Odd-even staggering in fragment yields

After the transmission efficiencies have been corrected for $T_z = -3/2$ and $T_z = -1$ nuclides, one can obtain the measured production-yield values, as shown in Fig. 2(a). A very evident OES is observed for the yields of both $T_z = -3/2$ nuclei and $T_z = -1$ nuclei, while the OES in the former is much stronger than that in the latter. For $T_z = -3/2$ nuclei, the largest value of the ratio between the yields of neighboring even- and odd-Z nuclei is about 5. For $T_z = -1$ nuclei, a sharp drop of fragment yields is observed around $Z = 20$ and thus the strongest OES is reached near this closed shell.

To quantitatively study the OES-FY, we can calculate the magnitudes of the OES from the measured production yields, according to Eq. (1). The open and filled red points in Fig. 2(b) show the calculated magnitudes of the OES for four consecutive yields of $T_z = -3/2$ and $T_z = -1$ nuclei, respectively, which were measured in this experiment. As shown in Fig. 2(b), the magnitude of the OES is much larger for $T_z = -3/2$ nuclei than $T_z = -1$ nuclei with the same Z. For the former, the magnitude tends to decrease and then increase slightly as Z increases. For the latter, the magnitude is almost a constant (20%) when $Z \leqslant 16$ and tends to increase as Z increases from 22 to higher atomic numbers. For $T_z = -1$

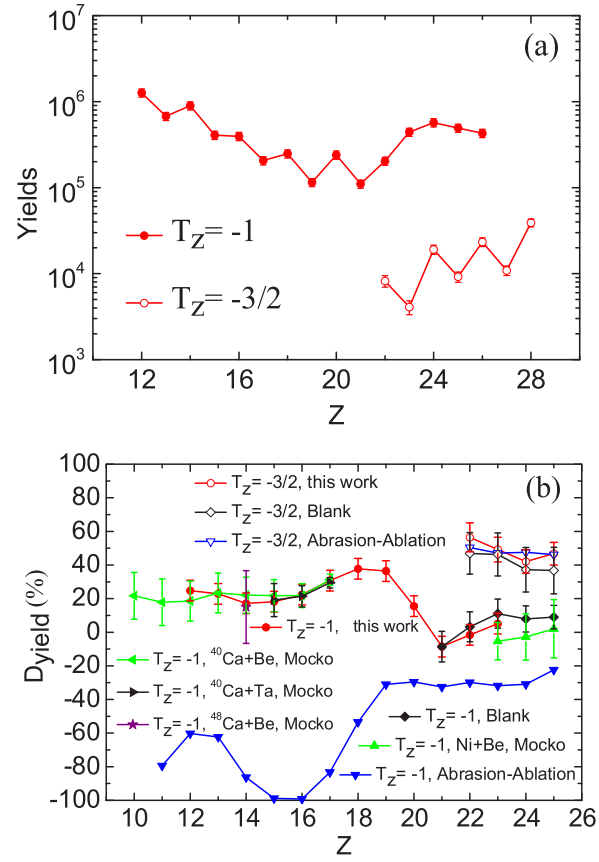

FIG. 2. (a) Yields of $T_z = -3/2$ and $T_z = -1$ nuclei measured in this ^{58}Ni fragmentation reaction experiment. The error is determined by the systematic uncertainty of the estimations of transmission efficiencies (10%) and the statistical uncertainty. Note that the yields are plotted on a logarithmic scale. (b) Magnitudes of the OES-FY for $T_z = -3/2$ and $T_z = -1$ nuclei measured in this experiment as well as those in other experimental data from the fragmentation of ^{58}Ni, ^{48}Ca, and ^{40}Ca projectiles reported in Refs. [1,3]. They are calculated according to Eq. (1). These experimental data are also compared with predictions of the abrasion-ablation model [29], where the evaporation parameters are similar to those used in Refs. [6,49,51].

nuclei measured in this work, the largest D_{yield} value of about 40% is reached near the closed shell $Z = 20$, which indicates that the shell structure has a very strong impact on the OES-FY. A similar shell impact was observed for yields of $T_z = -1/2$ nuclei around $Z = 20$ as well as $Z = 28$, which were measured in our previous work [6]. These experimental results reveal that the highest OES-FY along a constant T_z chain seems to be new sensitive shell evidence, especially for neutron-deficient nuclei close to the proton drip line.

One can also extract the magnitude of this OES-FY from other experimental data measured in different fragmentation reactions with different projectile-target combinations and investigate the projectile-target dependence of this OES-FY. Figure 2(b) also presents the magnitude calculated by Eq. (1) by using other experimental data; namely, the cross sections from ^{58}Ni +Be reactions at 650 MeV/nucleon reported by Blank *et al.* in Ref. [1] and the cross sections from ^{58}Ni +Be, ^{48}Ca +Be, ^{40}Ca +Be as well as ^{40}Ca +Ta reactions at

140 MeV/nucleon measured by Mocko *et al.* [3]. The OES in their measured cross sections of $T_z = -1$ and $T_z = -3/2$ nuclei is quantitatively calculated first by using this method. In their data, the shell impact cannot be studied for $T_z = -1$ nuclei around $Z = 20$ due to their limited experimental data. For both $T_z = -1$ nuclei and $T_z = -3/2$ nuclei, the magnitude of OES in their data is in very good agreement with that in our experimental data within the uncertainties, as shown in Fig. 2(b). This agreement between experimental data measured in different fragmentation reactions at different energies strongly supports our previous conclusion in Ref. [6] that this OES-FY almost does not depend on the projectile-target combinations. Additionally, this agreement indicates that the OES-FY is almost independent of the reaction energy between 140 and 650 MeV/nucleon.

The OES-FY in experimental data is also compared with that calculated from the theoretical abrasion-ablation model [29] for ^{58}Ni +Be reactions at 463 MeV/nucleon; see Fig. 2(b). In this model, the nuclei are assumed to be spheres from which the geometrical overlap is abraded. After the abrasion, the evaporation process is simulated in the code. The parameters used in the evaporation process are similar to those used in Refs. [6,49,51]. For instance, an average excitation energy of about 13 MeV per abraded nucleon and an effective proton evaporation radius [52] of 4 fm are used in the calculations. This model successfully reproduces the measured OES for $T_z = -3/2$ nuclei, as shown in Fig. 2(b). However, for $T_z = -1$ nuclei, the reversed OES ($D_{\text{yield}} < 0$) predicted by the model is not observed in the measured OES-FY and this model cannot reproduce the pronounced shell effect in the measured OES-FY. This large discrepancy may come from the choice of parameters or models used in the abrasion-ablation calculations. Thus, more investigations will be performed in the following to understand the measured OES-FY for both $T_z = -1$ nuclei and $T_z = -3/2$ nuclei.

B. Origin of odd-even staggering in fragment yields

So far, different fragmentation reaction models, e.g., the abrasion-ablation model [29] and the ISMM with secondary decay [27], have been tried to simulate fragmentation reactions, but they can hardly reproduce the measured OES in yields of fragments over a large range of Z [see, e.g., Fig. 2(b) and Refs. [6,15,27] for details]. Our previous study of OES-FY in the $T_z = 1/2$ and $T_z = -1/2$ nuclei indicates that the OES-FY seems to be dominated by the OES in the particle-emission threshold energy (PETE) [6], where all particle decays cease and the final fragments are formed in the evaporation process. In the following we will study the OES in PETE and check this conclusion by using our new experimental data for the $T_z = -1$ and $T_z = -3/2$ nuclei close to the proton drip line, where a strong OES-FY is observed.

When the Coulomb barrier is not taken into account, the PETE is the smallest value from either the proton separation energy S_p or the neutron separation energy S_n of this fragment, which was proposed to be an important quantity to calculate the fragment yields [53,54]. For $T_z = -1$ and $T_z = -3/2$ nuclei, the PETE value from the latest Atomic Mass Evaluation

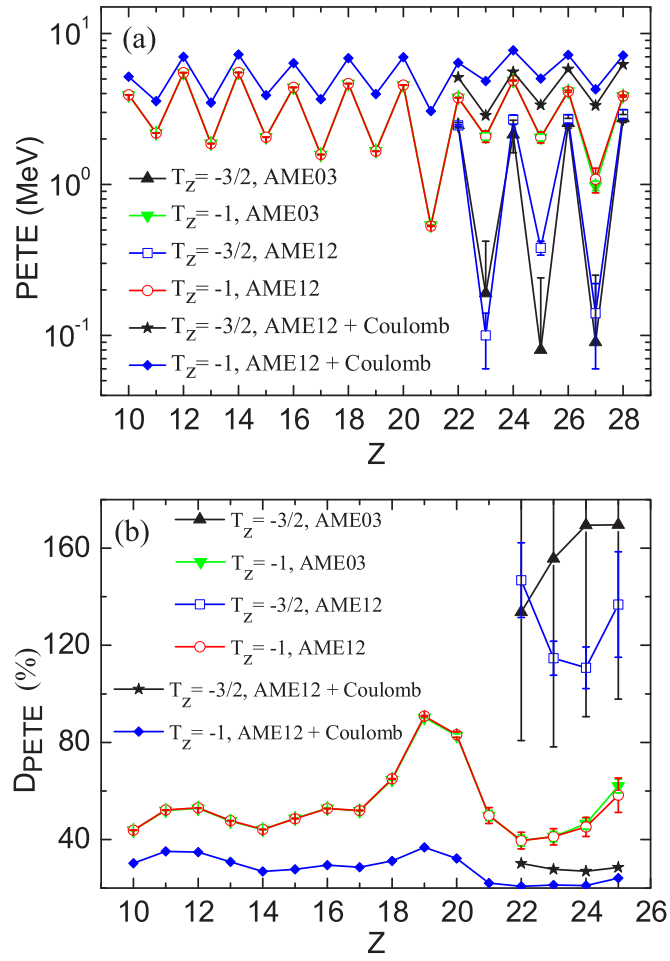

FIG. 3. (a) The particle-emission threshold energy (PETE) for $T_z = -3/2$ and $T_z = -1$ nuclei. The PETE value (S_p) from AME'03 [56] is compared with that from AME'12 [55] as well as with the sum of S_p from AME'12 and the Coulomb barrier. For ^{43}V, ^{47}Mn, and ^{51}Co, negative error bars of the PETE from AME'03 are out of range and are not shown. For $T_z = -3/2$ nuclei, the PETE from AME'03 is not measured by experiments, except for ^{45}Cr. In AME'12, the PETE is from experimental data, except for ^{52}Co and ^{53}Ni. In the case where the Coulomb barrier is considered, the error of PETE is not given since the Coulomb barrier is calculated from a theoretical model. (b) Magnitudes of the OES in PETE for $T_z = -3/2$ and $T_z = -1$ nuclei. They are calculated with Eq. (1), where yields are replaced by PETE values. For $T_z = -3/2$ nuclei, positive error bars of magnitudes calculated from AME'03 are out of range.

AME'12 [55] is compared with that from an older version AME'03 [56] in Fig. 3(a). They are in excellent agreement for $T_z = -1$ nuclei, but there is a large discrepancy between them for $T_z = -3/2$ nuclei, especially for the odd-Z ones. For $T_z = -3/2$ nuclei, this large discrepancy occurs because their PETE values (S_p) are from the theoretical extrapolation in AME'03, except for ^{45}Cr, while they are from experimental data in AME'12, except for ^{53}Ni. The PETE value of ^{52}Co is from the theoretical extrapolation both in AME'12 and in AME'03. The PETE value in Fig. 3(a) shows a significant OES, which is similar to the OES-FY in Fig. 2(a). Obviously,

the OES for $T_z = -3/2$ nuclei is much stronger than that for $T_z = -1$ nuclei. For the latter, the highest OES in PETE is observed near the closed shell $Z = 20$.

We can also calculate the magnitude of OES in PETE by using Eq. (1), where the yields Y are replaced by the corresponding PETE values. The calculated magnitude values are shown in Fig. 3(b). When the Coulomb barrier is not considered, although the OES in PETE (S_p) is much stronger than the OES-FY, they show remarkable similarities and present almost the same evolution pattern, as presented in Figs. 3(b) and 2(b). The magnitude of OES in PETE is larger for $T_z = -3/2$ nuclei than that for $T_z = -1$ nuclei with the same Z. For the latter, the magnitude is almost a constant as $10 < Z \leqslant 16$ and tends to increase when Z increases from 22 to 25. In addition, the largest magnitude is reached near the closed shell $Z = 20$. For the former, the magnitude of OES in PETE from AME'12 tends to decrease and then increase as Z increases, which is similar to that observed in the magnitude of OES-FY. But this tendency is not seen in the magnitude of OES in PETE from AME'03, which is obtained from theoretical extrapolation. The above results demonstrate that the OES-FY can be applied to check the PETE (separation energies) predicted by theoretical models, especially for those nuclei close to the drip lines, where the mass measurement is not yet reachable.

After the main source of OES has been studied, the proton Coulomb barrier, which varies smoothly with Z along a constant T_z chain, is also added into the PETE. In this case, the PETE value of $T_z = -1$ and $T_z = -3/2$ nuclei is the sum of S_p and the effective Coulomb barrier ($S_p + V_c$), see filled diamonds and stars in Fig. 3(a). The effective Coulomb barrier V_c is calculated by using a very simple theoretical model [50,52]:

$$V_c(Z,A) = \frac{1.44(Z-1)}{1.22[(A-1)^{1/3}+1]+6\ \mathrm{fm}}, \qquad (3)$$

where Z and A are the atomic and mass numbers, respectively. It is obvious that the smooth Coulomb barrier tends to decrease the OES in PETE, especially for $T_z = -3/2$ nuclei with very small S_p values, as shown in Fig. 3(a). However, this smooth factor does not change the staggering structure of PETE.

When the effective Coulomb barrier is added, the magnitude of OES in PETE ($S_p + V_c$) decreases substantially, particularly for $T_z = -3/2$ nuclei, while its evolution tendency is almost not changed; see filled diamonds and stars in Fig. 3(b). For $T_z = -1$ nuclei, the magnitude of OES in PETE is very close to that in fragment yields, as indicated in Figs. 3(b) and 2(b). For $T_z = -3/2$ nuclei, the magnitude of OES in PETE is a little smaller than that in fragment yields. This deviation may be caused by the choice of the Coulomb barrier model or parameters used in this model.

The above results demonstrate that the OES-FY is mainly originated from the OES in the minimum value of S_n and S_p, which are strongly affected by both pairing and shell effects. Additionally, our study reveals that the Coulomb barrier tends to decrease the OES in PETE, which is much closer to the OES-FY after the Coulomb barrier is considered in the PETE.

V. SUMMARY

In summary, a combination of a fragment separator and a storage ring at HIRFL has been applied to measure the yields of $T_z = -1$ and $T_z = -3/2$ nuclei, produced by ^{58}Ni fragmentation on a Be target at an energy of 463 MeV/nucleon. Measured yields of both $T_z = -1$ and $T_z = -3/2$ nuclides show a very evident OES. It is found that the highest OES-FY is reached near the closed shell $Z = 20$ for $T_z = -1$ nuclides due to the strong shell effect on the deduced OES-FY. A comparison of different experimental data reveals that this OES-FY is almost independent of the projectile-target combinations as well as the fragmentation energy between 140 and 650 MeV/nucleon.

To explore the origin of the OES-FY, the OES in PETE has also been studied. Our investigation supports the conclusion that OES-FY is mainly dominated by the OES in the nucleon separation energies. In addition, the OES in PETE is much closer to the OES-FY when the Coulomb barrier, which tends to decrease the OES in PETE, is taken into account.

ACKNOWLEDGMENTS

We would like to thank Dr. A. Stolz and Dr. T. Baumann for their help on the LISE++ program. This research was partially supported by the 973 Program of China (No. 2013CB834401), by the National Natural Science Foundation of China (Grants No. 10925526, No. 11035007, No. U1232208, No. 10675147, No. 10805059, No. 11135005, and No. 11075103), by the Project Extreme Light Infrastructure Nuclear Physics (ELI-NP) - Phase I, a project co-financed by the Romanian Government and the European Union through the European Regional Development Fund, by the CAS Pioneer Hundred Talents Program, by the BMBF grant in the framework of the Internationale Zusammenarbeit in Bildung und Forschung (Projekt-Nr. 01DO12012), by the Helmholtz-CAS Joint Research Group (HCJRG-108), by the External Cooperation Program of the Chinese Academy Sciences (Grant No. GJHZ1305), by the Max-Planck Society, by the ESF through EuroGENESIS program, and by HIC for FAIR.

[1] B. Blank *et al.*, Phys. Rev. C **50**, 2398 (1994).
[2] J. Kurcewicz *et al.*, Phys. Lett. B **717**, 371 (2012).
[3] M. Mocko *et al.*, Phys. Rev. C **74**, 054612 (2006).
[4] O. B. Tarasov *et al.*, Phys. Rev. Lett. **102**, 142501 (2009).
[5] O. B. Tarasov *et al.*, Phys. Rev. C **87**, 054612 (2013).
[6] B. Mei *et al.*, Phys. Rev. C **89**, 054612 (2014).
[7] C. N. Knott *et al.*, Phys. Rev. C **53**, 347 (1996).
[8] C. Zeitlin *et al.*, Phys. Rev. C **56**, 388 (1997).
[9] C. N. Knott *et al.*, Phys. Rev. C **56**, 398 (1997).
[10] C. X. Chen *et al.*, Phys. Rev. C **56**, 1536 (1997).
[11] L. B. Yang *et al.*, Phys. Rev. C **60**, 041602(R) (1999).
[12] E. M. Winchester *et al.*, Phys. Rev. C **63**, 014601 (2000).

[13] A. Leistenschneider *et al.*, Phys. Rev. C **65**, 064607 (2002).
[14] E. Geraci *et al.*, Nucl. Phys. A **732**, 173 (2004).
[15] M. V. Ricciardi *et al.*, Nucl. Phys. A **733**, 299 (2004).
[16] G. Iancu, F. Flesch, and W. Heinrich, Radiat. Meas. **39**, 525 (2005).
[17] C. Zeitlin *et al.*, Phys. Rev. C **77**, 034605 (2008).
[18] M. Huang *et al.*, Phys. Rev. C **81**, 044620 (2010).
[19] M. Huang *et al.*, Phys. Rev. C **82**, 054602 (2010).
[20] M. V. Ricciardi, K. H. Schmidt, and A. Kelić-Heil, arXiv:1007.0386.
[21] J. Su, F.-S. Zhang, and B.-A. Bian, Phys. Rev. C **83**, 014608 (2011).
[22] I. Lombardo *et al.*, Phys. Rev. C **84**, 024613 (2011).
[23] M. D'Agostino *et al.*, Nucl. Phys. A **861**, 47 (2011).
[24] G. Casini *et al.*, Phys. Rev. C **86**, 011602(R) (2012).
[25] K. Hagino and H. Sagawa, Phys. Rev. C **85**, 037604 (2012).
[26] M. D'Agostino *et al.*, Nucl. Phys. A **875**, 139 (2012).
[27] J. R. Winkelbauer, S. R. Souza, and M. B. Tsang, Phys. Rev. C **88**, 044613 (2013).
[28] R. J. Charity, Phys. Rev. C **58**, 1073 (1998).
[29] J. J. Gaimard and K. H. Schmidt, Nucl. Phys. A **531**, 709 (1991).
[30] N. L. Calleya, S. R. Souza, B. V. Carlson, R. Donangelo, W. G. Lynch, M. B. Tsang, and J. R. Winkelbauer, Phys. Rev. C **90**, 054616 (2014).
[31] B. L. Tracy *et al.*, Phys. Rev. C **5**, 222 (1972).
[32] A. Olmi and S. Piantelli, Eur. Phys. J. A **51**, 154 (2015).
[33] Y. A. Litvinov *et al.*, Nucl. Instrum. Methods Phys. Res., Sect. B **317**, 603 (2013).
[34] B. Mei *et al.*, Phys. Rev. C **92**, 035803 (2015).
[35] X. L. Tu *et al.*, Phys. Scr. **T166**, 014009 (2015).
[36] Y. A. Litvinov, *RIB Physics with Storage Rings* (2015).
[37] J. W. Xia *et al.*, Nucl. Instrum. Methods Phys. Res., Sect. A **488**, 11 (2002).
[38] M. Hausmann *et al.*, Nucl. Instrum. Methods Phys. Res., Sect. A **446**, 569 (2000).
[39] M. Hausmann *et al.*, Hyperfine Interact. **132**, 289 (2001).
[40] B. Sun *et al.*, Nucl. Phys. A **812**, 1 (2008).
[41] B. Franzke, H. Geissel, and G. Münzenberg, Mass Spectrom. Rev. **27**, 428 (2008).
[42] F. Bosch, Y. A. Litvinov, and T. Stöhlker, Prog. Part. Nucl. Phys. **73**, 84 (2013).
[43] B. Mei *et al.*, Nucl. Instrum. Methods Phys. Res., Sect. A **624**, 109 (2010).
[44] P. Shuai *et al.*, Phys. Lett. B **735**, 327 (2014).
[45] X. L. Tu *et al.*, Phys. Rev. Lett. **106**, 112501 (2011).
[46] X. L. Tu *et al.*, Nucl. Instrum. Methods Phys. Res., Sect. A **654**, 213 (2011).
[47] Y. H. Zhang *et al.*, Phys. Rev. Lett. **109**, 102501 (2012).
[48] X. L. Yan *et al.*, Astrophys. J. Lett. **766**, L8 (2013).
[49] T. Yamaguchi *et al.*, Phys. Rev. C **74**, 044608 (2006).
[50] O. Tarasov and D. Bazin, Nucl. Instrum. Methods Phys. Res., Sect. B **266**, 4657 (2008).
[51] A. Stolz *et al.*, Phys. Lett. B **627**, 32 (2005).
[52] J. Benlliure *et al.*, Eur. Phys. J. A **2**, 193 (1998).
[53] J. Hüfner, C. Sander, and G. Wolschin, Phys. Lett. B **73**, 289 (1978).
[54] X. Campi and J. Hüfner, Phys. Rev. C **24**, 2199 (1981).
[55] M. Wang *et al.*, Chin. Phys. C **36**, 1603 (2012).
[56] G. Audi, A. H. Wapstra, and C. Thibault, Nucl. Phys. A **729**, 337 (2003).